International Journal of Heat and Mass Transfer 52 (2009) 1276–1283

Contents lists available at ScienceDirect

International Journal of Heat and Mass Transfer

journal homepage: www.elsevier.com/locate/ijhmt

Development of a multiple layer vacuum insulation chip

Il Seob Yoon, Tae-Ho Song *

School of Mechanical, Aerospace and Systems Engineering, Korea Advanced Institute of Science and Technology, Kusong-dong 373-1, Yuseong-gu, Daejon, Republic of Korea

ARTICLE INFO

Article history:
Received 15 January 2008
Received in revised form 22 August 2008
Available online 14 November 2008

ABSTRACT

Advent of micro thermal devices such as lab-on-a-chip and micro heat pump necessitates development of highly effective insulation chips or layers. This paper reports the development of a vacuum insulation chip (VIC) having very low effective thermal conductivity and very small thickness. Fifty nanometer thickness metal coating on both sides of an LCD glass chip and 5 μm vacuum gap are stacked in a series to decrease the heat transfer by radiation. An array of support legs is necessary to maintain the structure under the atmospheric pressure. Design of VIC involves trade-offs between the heat conduction through the multi-layer structure and the mechanical strength. A model to determine the actual design values is proposed. The results are in reasonable agreement with the more refined results using commercial numerical codes. Based on these results, a VIC of $32 \times 32 \times 1.88$ mm^3 is manufactured, and the effective thermal conductivity is measured by guarded hot plate method. The chip shows effective thermal conductivities of 0.0015 and 0.001 W/m K at vacuum levels of 1.33 and 0.24 Pa (N/m^2), respectively.

1. Introduction

Lately, new micro thermal devices such as lab-on-a-chip and micro heat pump are being developed. To obtain the optimum performance, these devices require highly efficient insulation methods to be used under atmospheric pressure in an extremely confined space. An insulation chip to come up with this requirement is highly required.

This work is motivated by these needs and reports the development of a VIC. A sophisticated design of the insulation layer is sought for. Among the insulation methods, vacuum insulation effectively eliminates the gas conduction in the enclosure. In addition, low emittance coatings on the inner surfaces result in very low levels of radiation heat transfer. Spinnler et al. [1,2], Scurlock and Saull [3], Krishnaprakas et al. [4] and Jacob et al. [5] investigate theoretical or experimental study to design the multi-layer thermal insulation systems by using spacer (such as micro porous media and aluminum foil). Collins et al. [6–8] have practically developed single layer double pair vacuum insulation panels (VIP) using tiny support crystals. Still, their thermal insulation systems have a fairly large gap size and they do not have to consider the wave interference or tunneling effect by the evanescent wave which comes into play when the gap size is further reduced. Liang and Han [9] investigate the numerical heat conduction and thermal radiation at different gap sizes and temperatures for two parallel blackbody plates considering the wave interference and tunneling effect. Whale and Cravalho [10,11] have derived proximity functions that provide a simple and elegant means to account for the tunneling effect. Yet, tunneling effect through real materials in multi-layer remains to be solved for.

This research is concerned with multi-layer thermal insulation in micro scale, aiming at the development of a VIC. An innovative idea of the insulation layer is proposed. Formulations are introduced to analyze the radiation transfer in a very thin gap as well as the conduction and the structure stress. Based on the results of theoretical studies, a VIC with a few millimeters thicknesses is manufactured. The effective thermal conductivity is experimentally measured.

2. Design and analysis

2.1. Conceptual design

The VIC to be developed is a multi-layer insulation chip with vacuum gaps between multiple plates. Fig. 1 shows the conceptual configuration of the VIC. In this figure, three glass plates are layered and two vacuum gaps are provided between them. Many materials are reviewed as candidates of the plate material. A material with low thermal conductivity and high strength is desirable, as shall be shown later. A 0.625 mm thick LCD panel glass, Corning® EAGLE^{2000TM} AMLCD glass, is finally selected (see Table 1 for the properties).

To withstand the atmospheric pressure, support legs are to be installed in an array. Square array of support legs is formed by etching the LCD glass plate. The distance between the legs is to be determined later together with the diameter and the gap size. With a small size chip in mind, the size of the chip is taken as 32 mm by 32 mm. The square formed by the leg in the upper gap is arranged in a staggered manner in the lower gap so that the thermal

* Corresponding author. Tel.: +82 42 869 3032;fax: +82 42 869 3210.
E-mail address: thsong@kaist.ac.kr (T.-H. Song).

0017-9310/$ - see front matter © 2008 Elsevier Ltd. All rights reserved.
doi:10.1016/j.ijheatmasstransfer.2008.08.028

Nomenclature

A	area of block heater, m^2
C_1, C_2	constants of the Planck function, ($= 3.7419 \times 10^{-16}$ W m^2 and 1.4388×10^{-2} m K)
d	diameter of the support leg, m
E	Young's modulus of elasticity, N/m^2
E_b	blackbody emissive power, W/m^2
h	heat transfer coefficient, W/m^2 K
k	thermal conductivity, W/m K
k_0	free molecular conductivity at 0°C, W/K N
L	vacuum insulation thickness, m
M	molecular weight
M_j	characteristic matrix of each layer
M_o	overall characteristic matrix
n	refractive index
P	pressure, N/m^2
Q	thermal input power, W
R	thermal resistance, K/W
S	safety factor
T	temperature, K
t	glass plate thickness, m
W	distance between support legs, m

Greek symbols

α	absorptivity
α_{gas}	accommodation coefficient
δ	layer thickness, m
θ	incidence angle, radian
λ	wavelength, m
ν	poisson's ratio
ρ	reflectivity
σ_{comp}	compression stress, N/m^2
σ_{dc}	dc-conductivity, $\Omega^{-1}m^{-1}$
σ_{yield}	yield stress, N/m^2
τ	transmissivity
τ_{shear}	shear stress, N/m^2

Subscripts

atm	atmospheric pressure
bh	block heater
c	cold temperature
cal	calculation
chip	VIC
eff	effective
env	envelop
exp	experiment
g	glass
gas	gas conduction
h	hot temperature
mc	metal coating
sup	support leg
TE	transverse electric wave
TM	transverse magnetic wave
λ	spectral
v	vacuum

conduction path from the uppermost to the lowermost plate should be the longest. By making so, the conduction resistance may be maximized and increased multi-layer stacking is made possible.

Our consideration regarding the insulation performance is primarily concerned with radiation exchange across the gap, conduction through the support legs and conduction through the residual gas under moderate vacuum. The former two are strictly treated through theoretical calculations and the last is only conceptually examined.

2.2. Radiation heat transfer

2.2.1. Analysis

As mentioned earlier, vacuum layers and metal coatings on the inner surface of one or both glass plates are very effective in thermal insulation. To analyze the radiation heat transfer, the structure is modeled as a stack of stratified multi-layer as shown in Fig. 2. Each layer has thickness δ_i and refractive index n_i.Consider a plane electromagnetic wave propagating through the stratified medium with an incidence angle θ_1. The wave may be linearly polarized with its electric field vector perpendicular to the plane of incidence (transverse electric wave; TE wave), or with its magnetic field vector perpendicular to the plane of incidence (transverse magnetic wave; TM wave). The characteristic matrix of electromagnetic wave propagation of each layer is seen to be the following Eq. (1) for a TE wave [12]. For a TM wave, the same equations hold with $p_j = n_j \cos\theta_j (j = 2,3,\cdots l-1)$ replaced by $q_j = \cos\theta_j / n_j$.

$$M_j = \begin{pmatrix} \cos\left(\frac{2\pi}{\lambda}\delta_j n_j \cos\theta_j\right) & -\frac{i}{p_j}\sin\left(\frac{2\pi}{\lambda}\delta_j n_j \cos\theta_j\right) \\ -ip_j \sin\left(\frac{2\pi}{\lambda}\delta_j n_j \cos\theta_j\right) & \cos\left(\frac{2\pi}{\lambda}\delta_j n_j \cos\theta_j\right) \end{pmatrix} \quad (1)$$

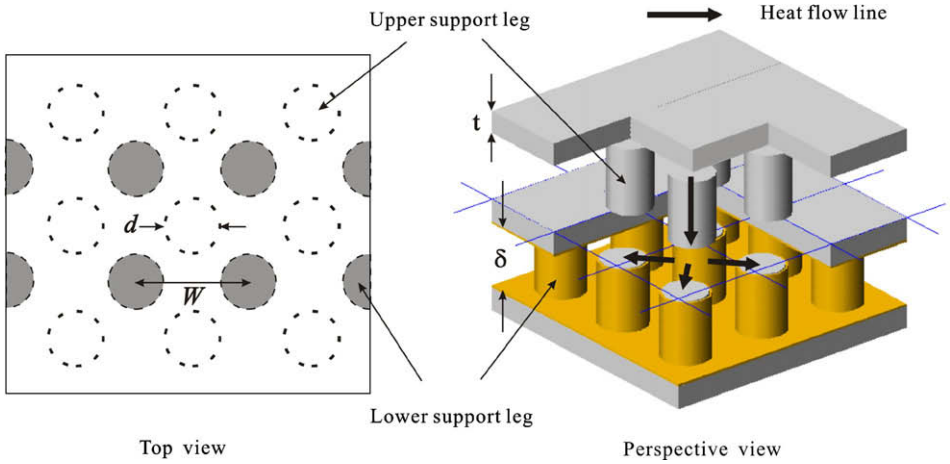

Fig. 1. Concept of multilayer structure.

Table 1
Properties of the used glass plate

Corning® EAGLE^{2000TM} AMLCD glass substrates			
Yield strength (MPa)	Compression strength (GPa)	Shear strength (GPa)	Young's modulus (GPa)
173.2	10.0	30.0	70.9
Thermal conductivity (W/m K)	Thermal expansion coefficient at 0–300 °C (/°C)		Poisson's ratio
0.89	31.8×10^{-7}		0.23

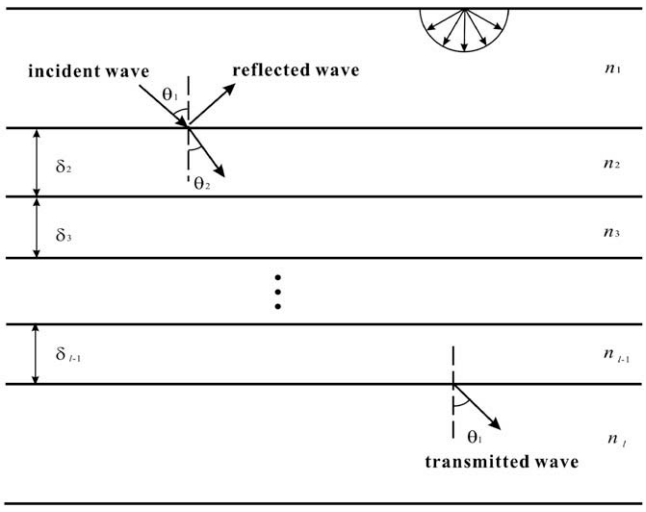

Fig. 2. A simplified multilayer structure.

The overall characteristic matrix of the stratified medium is

$$M_o = M_2 M_3 \cdots M_{l-2} M_{l-1} = \begin{pmatrix} m_{11} & m_{12} \\ m_{21} & m_{22} \end{pmatrix} \tag{2}$$

It can be obtained the reflectivity and transmissivity of the stratified medium for the TE wave from Eqs. (3) and (4).

$$\rho_{\mathrm{TE},\lambda}(\theta) = \left| \frac{(m_{11} + m_{12}p_l)p_1 - (m_{21} + m_{22}p_l)}{(m_{11} + m_{12}p_l)p_1 + (m_{21} + m_{22}p_l)} \right|^2 \tag{3}$$

$$\tau_{\mathrm{TE},\lambda}(\theta) = \frac{p_l}{p_1} \left| \frac{2p_1}{(m_{11} + m_{12}p_l)p_1 + (m_{21} + m_{22}p_l)} \right|^2 \tag{4}$$

When the incident light is randomly polarized, using Eqs. (3, 4) and q_j, it can be calculated the reflectivity and transmissivity as,

$$\rho_\lambda(\theta) = \frac{\rho_{\mathrm{TE},\lambda}(\theta) + \rho_{\mathrm{TM},\lambda}(\theta)}{2} \tag{5}$$

$$\tau_\lambda(\theta) = \frac{\tau_{\mathrm{TE},\lambda}(\theta) + \tau_{\mathrm{TM},\lambda}(\theta)}{2} \tag{6}$$

Usually, when the incidence angle exceeds the critical angle, the incident light is reflected perfectly. However, in case the thickness is of the order of the wavelength and the light propagates from an optically denser medium into less dense one beyond the critical angle, partial propagation (evanescent wave) occurs due to the tunneling effect. Radiation heat transfer can be increased by the evanescent wave. Eq. (7) shows how we can calculate this effect. The calculated results are verified through Eq. (8).

$$n_{j+1} \cos\theta_{j+1} = i\sqrt{n_j^2 \sin^2\theta_j - n_{j+1}^2} \tag{7}$$

$$\rho + \tau = 1 \tag{8}$$

In case the stratified medium includes metal layers, since the refractive index of metal layer is a complex one, Eqs. (1)–(4) are calculated by replacing n_j by $\tilde{n}_j = n_j(1 + ik_j) = u_j + iv_j$. It can be expressed u_j and v_j as

$$2u_j^2 = A + \sqrt{A^2 + 4n_j^4 k_j^2}, \quad 2v_j^2 = -A + \sqrt{A^2 + 4n_j^4 k_j^2} \tag{9}$$

(where, $A = n_j^2(1 - k_j^2) - n_{j-1}^2 \sin^2\theta_{j-1}$).

Also, since the refractive index of a metal is heavily dependent on the wavelength, we use the data of Palik [13] and, for long wavelength, the Hagen–Rubens relation [14], i.e., Eq. (10). Absorptivity is then calculated using Eq. (11).

$$n_j \approx n_j k_j = \sqrt{30\lambda \cdot \sigma_{dc}}, (\text{where, } \lambda \text{ in m, } \sigma_{\mathrm{dc}} \text{ in } \Omega^{-1}\mathrm{m}^{-1}) \tag{10}$$

$$\alpha = 1 - \rho - \tau \tag{11}$$

Finally, we introduce the total reflectivity and transmissivity that represent the integrated average reflectivity and transmissivity over the hemisphere over the spectral blackbody emissive power $E_{b,\lambda}$. In other words, the uppermost and lowermost boundaries are assumed to be subject to external blackbody radiation. Furthermore, we investigate the effect of a specific layer thickness δ while the other parameters are fixed. We formally obtain the following expressions.

$$E_{b,\lambda} = \frac{C_1}{n^2\lambda^5(e^{C_2/n\lambda T} - 1)} \tag{12}$$

$$\rho_\lambda = \int_{\lambda_1}^{\lambda_2} 2\sin\theta \cdot \cos\theta \cdot \rho_\lambda(\theta)\mathrm{d}\theta \equiv f_1\left(\frac{\lambda}{\delta}, n\right) \tag{13}$$

$$\rho_{\mathrm{total}} = \frac{\int_{\lambda_1}^{\lambda_2} E_{b,\lambda} \cdot \rho_\lambda \mathrm{d}\lambda}{\int_{\lambda_1}^{\lambda_2} E_b \mathrm{d}\lambda} \tag{14}$$

$$\tau_\lambda = \int_{\lambda_1}^{\lambda_2} 2\sin\theta \cdot \cos\theta \cdot \tau_\lambda(\theta)\mathrm{d}\theta \equiv f_2\left(\frac{\lambda}{\delta}, n\right) \tag{15}$$

$$\tau_{\mathrm{total}} = \frac{\int_{\lambda_1}^{\lambda_2} E_{b,\lambda} \cdot \tau_\lambda \mathrm{d}\lambda}{\int_{\lambda_1}^{\lambda_2} E_b \mathrm{d}\lambda} \tag{16}$$

From Eqs. (12)–(16) and using parameter $\xi \equiv n\lambda\, T/C_2$, Eqs. (17) and (18) are obtained. The dimensionless parameter $C_2/nT\delta$ which is related to the gap thickness and the temperature is shown in these equations.

$$\rho_{\mathrm{total}} = \int_0^\infty f_1\left(\frac{C_2\xi}{nT\delta}, n\right) \cdot \frac{15}{\pi^4} \cdot \frac{1}{\xi^5(e^{1/\xi} - 1)} \mathrm{d}\xi \equiv g_1\left(\frac{C_2}{nT\delta}, n\right) \tag{17}$$

$$\tau_{\mathrm{total}} = \int_0^\infty f_2\left(\frac{C_2\xi}{nT\delta}, n\right) \cdot \frac{15}{\pi^4} \cdot \frac{1}{\xi^5(e^{1/\xi} - 1)} \mathrm{d}\xi \equiv g_2\left(\frac{C_2}{nT\delta}, n\right) \tag{18}$$

2.2.2. Calculation results

Using the above equations, it can be calculated the transmissivity, reflectivity and absorptivity of the stratified medium including glass plate, vacuum gap and metal coating. We set the temperature T = 300 K and refractive index of glass n = 1.5. The uppermost surface is exposed to infinitesimally hotter blackbody radiations than the lowermost one.

When no metal coating is employed, the transmissivity is shown in Fig. 3, where only the gap size is varied. We find that radiation transmissivity across the stratified structure increases rapidly to unity as the vacuum gap size δ_v decreases below the typical wavelength of thermal radiation, which is caused by the tunneling effect. Also, when the vacuum gap size increase, it decreases to a lower asymptotic value which is between 0.3 and 0.4. Note that this limiting value is identical with that neglecting the evanescent wave. Transmissivity increases moderately with a small number of layers, while it approaches an asymptotic limit with greater number of layers. The calculated effective radiative

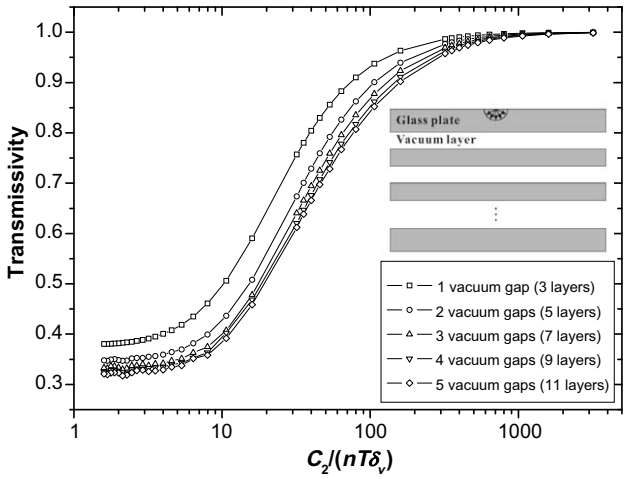

Fig. 3. Vacuum gap size and layer number effects for no metal coating (glass thickness fixed at 0.625 mm ; absorptivity is zero for this case).

conductivity of the layers comprising two vacuum gaps of 5 μm is about 3.2×10^{-3} W/m K. This is not low enough so we turn to the case of metal coating on the glass plates.

The transmissivity and absorptivity of multi-layer structure with metal coating are shown in Fig. 4. We assume that both of the vacuum sides are coated with aluminum and vacuum gap size is fixed at 5 μm. As shown in Fig. 4, we find that the thermal transmission is nearly zero as the metal coating thickness δ_{mc} increase. For the case of metal coating thickness 0.05 μm and two vacuum gaps, the effective radiative conductivity can be lowered to about 8.31×10^{-11} W/m K at room temperature. Considering only the radiative heat transfer, the thermal insulation performance is tremendously improved by employing metal coating with thickness greater than 0.05 μm.

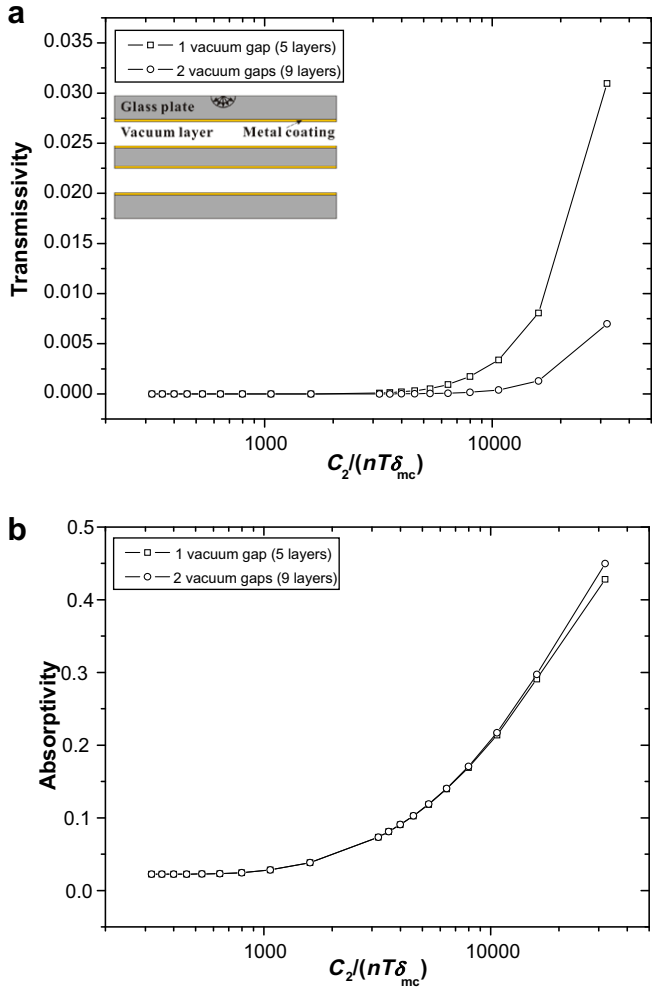

Fig. 4. Effect of metal coating thickness (glass thickness = 0.625 mm, vacuum gap size = 5 μm, coating metal = aluminum). (a) Transmissivity, (b) absorptivity.

Reflectivity, transmissivity and absorptivity have been calculated for many cases depending on which sides are metal coated. After an extensive calculation, the vacuum gap size and the metal coating thickness are fixed at 5 and 0.05 μm, respectively. Aluminum is coated only on the two surfaces of the middle LCD glass plate in the second vacuum gap structure. By taking these values, the radiative heat transfer is suppressed to a negligible order.

Note that the current results are not varied appreciably by changing the glass thickness moderately since the glass thickness is much greater than the IR wavelength.

2.3. Stress analysis

VIC's with multi-layer structure must withstand the atmospheric pressure. Thus the support legs are conceived and they must be minimally installed to minimize the thermal conduction through them.

Parameters to design the system are: distance between the support legs W, diameter d of a support leg, its height δ_v and thickness of the glass plate t. Note that the vacuum gap size δ_v is also the height of the support leg. Since we have already determined δ_v and t, only W and d remain to be determined. Considering the possible failure modes of materials [15], Eqs. (19)–(22) are obtained as;

$$W \leqslant \sqrt{\frac{2\sigma_{yield}}{3\,P_{atm}\cdot S}}\cdot t, \quad \text{from bending of glass plate.} \tag{19}$$

$$W \leqslant \sqrt{\frac{\pi\sigma_{comp}}{4\,P_{atm}\cdot S}}\cdot d, \quad \text{from support leg compression.} \tag{20}$$

$$W \leqslant \sqrt{\frac{\pi\tau_{shear}}{P_{atm}\cdot S}}\sqrt{d\cdot t}, \quad \text{from shearing of glass plate by the support leg.} \tag{21}$$

$$d^4 \geqslant \frac{16\,P_{atm}\cdot S}{\pi^3 E}\delta_v^2 W^2, \quad \text{from buckling of support leg.} \tag{22}$$

Among these, Eqs. (19) and (20) usually determine the real dimensions. In addition, even if it may not cause failure, deflection of the glass plate may eventually make two plates contact each other, which increases thermal conduction significantly. The maximum allowable deflection of the glass plates is the gap size and it gives another criterion

$$\delta_v \geqslant \frac{5}{32}\frac{S\cdot P_{atm} W^4}{E\cdot t^3} \tag{23}$$

Using these criteria, W and t shall be determined later.

2.4. Conduction analysis

Two heat conduction processes contribute to heat transfer through the evacuated insulation structure. They are conduction by the residual gas in the gap and that through the support legs.

2.4.1. Conduction by the residual gas

The thermal conductivity of gas is independent of pressure over a wide range of pressures. However, when the gas pressure is so low that the molecular mean free path is about equal to or greater than the gap size, the conductivity is dependent on the pressure.

The effective heat transfer coefficient h_{gas} in this pressure may be written as [16],

$$h_{gas} = 133.32\alpha_{gas} \cdot k_0 \left(\frac{273}{T}\right)^{1/2} \cdot P \ \mathrm{W/m^2\,K}(P \text{ in } \mathrm{N/m^2}, T \text{ in K}) \quad (24)$$

The accommodation coefficient α_{gas} is defined as the ratio of the energy actually transferred between impinging gas molecules and a surface, and the energy transferred if the impinging molecules reach a complete thermal equilibrium with the surface. The gas pressure P is in Pa (N/m^2) and the free molecular conductivity k_0 at 0°C is given by,

$$k_0 = \frac{1.10}{M^{1/2}} \frac{\gamma+1}{\gamma-1} \quad (25)$$

For air ($\gamma = 1.4$, $M = 28.98$) at $T = 300$ K and $\alpha = 0.8$ in contact with aluminum [16], Eq. (24) is replaced by:

$$h_{gas} = 0.94 \cdot P \ \mathrm{W/m^2K} \quad (26)$$

Note that there are four surfaces facing the gap for the proposed three-plate two-gap VIC, each of which has h_{gas} as given by this equation. Also, it should be always checked if δ is greater than the mean free path λ_{mean} so that we can apply these equations. For air, at room temperature, the simple formula [16]

$$\lambda_{mean} = \frac{6.67 \times 10^{-3}}{P} \quad (27)$$

can be used, with P in N/m^2 and λ in m. It can be seen that at $P = 1.33$ N/m^2, $\lambda_{mean} = 5$ mm.

2.4.2. Conduction through the support legs

A comprehensive analysis of the heat transfer through the support legs has been made by Collins et al. [7,8]. In their works, thermal resistance of support leg for a cylindrical glass support leg of diameter d and height δ may be written as

$$R_{sup} = \frac{1 + 4\delta_v/\pi d}{k_g d} \quad (28)$$

Note that the glass plate is already very thick compared with other dimensions and it has negligible thermal resistance except near the contact spot. Glass plate resistance is roughly $t/k_g W^2$ per plate. Then, including the plate resistance, the total thermal resistance R_{total} of our structure shown in Fig. 1 is written as the sum of the thermal resistances of glass plates and support legs.

$$R_{total} = \frac{t}{k_g W^2} \times 3 + \frac{1 + 4\delta_v/\pi d}{k_g d} \times 2 \quad (29)$$

Following the equation shows the heat transfer coefficient h_{sup} of the proposed structure with a square array of support legs of separation W.

$$h_{sup} = \frac{1}{R_{total} \cdot W^2} \quad (30)$$

Combining Eqs. (26) and (30), we obtain the effective thermal conductivity k_{eff} as for the three-plate two-gap VIC,

$$k_{cal,eff} = (h_{gas}/4 + h_{sup}) \cdot L_{chip} \quad (31)$$

2.5. Actual dimensioning and numerical validation

Although many small support legs to withstand the atmospheric pressure are required, the distance between support legs must be maximal to reduce the conduction by structure. Also, the diameter of support legs must be minimal. The safety factor is fixed to 2. Using the properties of glass in Table 1, the actual values of W and d which can withstand the atmospheric pressure are calculated. Eqs. (19) and (23) are set to equality to determine two candidates of W, among which the minimum is taken. Then d is determined from Eq. (20). Inequalities (21) and (22) are verified to be satisfied. Table 2 shows the calculated W and d together with other given data.

Table 2
Design parameter values

W (mm)	d (mm)	δ_v (mm)	t (mm)	S
7.5	0.06	0.005	0.625	2

To validate the preceding analytical predictions, numerical codes are applied to the designed structure. First, grid generation for 32 × 32 mm VIC chip is conducted using TrueGrid® and Gambit. For the stress analysis, a FEM commercial program (ABAQUS) is used. It is assumed that an uniform pressure ($P = 101.325$ N/m^2) is acting on the outer surfaces of upper plate. Though not shown here in detail, the stresses in the structure are close to the analytical predictions. Also, a CFD commercial code (Fluent) is used to cross-check the results of the conduction analysis. It is assumed that all faces are insulated and heat is transferred from upper-most surface to lower-most surface only through the support legs (in other words, residual gas conduction is neglected). The effective thermal conductivity using Eq. (30) is also compared with the results using Fluent in Table 3. From the results, we can say that Eq. (30) predicts within 5% error in average.

3. Development and performance test

3.1. VIC manufacture

A schematic diagram and the photograph of the manufactured VIC are shown in Fig. 5. Total of 9 VICs is shown here. We cut the LCD glass plates using scriber (a glass cutting machine). To smoothen the flaw at the cutting edge, brief thermal treatment is performed.

To make the support leg on glass plate surface, photo-resist coating in size of the support leg diameter is made. The glass plate is then etched in 5 μm depth by using etching solution, etchall (B& B products, Inc.). An earlier trial with dry-etching by MEMS technique shows slightly better results at the expense of increased etching time and cost, which is not used anymore. Fig. 6 shows the photograph of etched glass plate using SEM.

As mentioned before, the middle glass plate surfaces are coated with aluminum, 0.05 μm thick, using a sputtering system. Since aluminum has very low vapor pressure at 300 K [16], the aluminum sublimation problem which may occur at elevated temperatures is not considered here. To form the vacuum space, glass housing enveloping the 9 VIC's is manufactured using an UV cure adhesives (Beijing Tonsan New Materials & Tech. Co.). Total size of VIC assembly is 98 × 98 mm^2 with thickness 3.13 mm. Torr Sealant (Varian, Inc.) is used to maintain the vacuum. One millimeter diameter SUS tube is connected at glass housing side surface to the vacuum pump.

Table 3
Comparison of the heat transfer coefficients obtained by Eq. (30) and Fluent

Parameter				Heat transfer coefficient using Eq. (30) (W/m^2 K)	Heat transfer coefficient using Fluent (W/m^2 K)
W (mm)	d (mm)	δ_v (mm)	t (mm)		
7.5	0.06	0.005	0.625	0.43	0.45
6.4	0.06	0.005	0.625	0.59	0.64
6.5	0.052	0.005	0.625	0.49	0.49
5.5	0.044	0.005	0.625	0.56	0.52

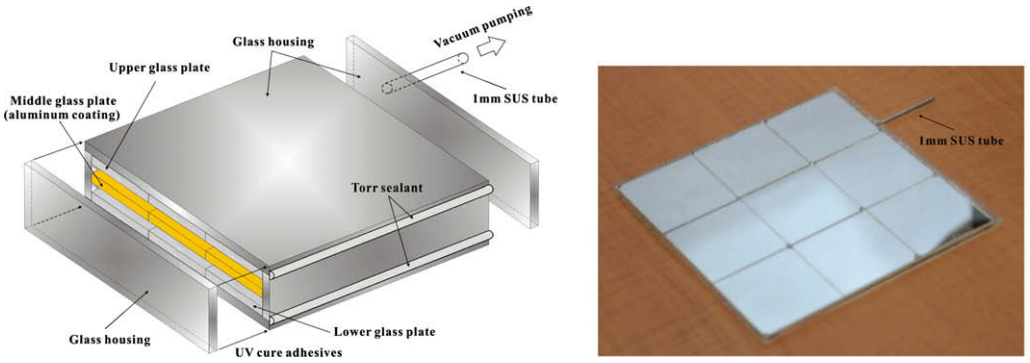

Fig. 5. Schematic diagram and photograph of the vacuum insulation panel.

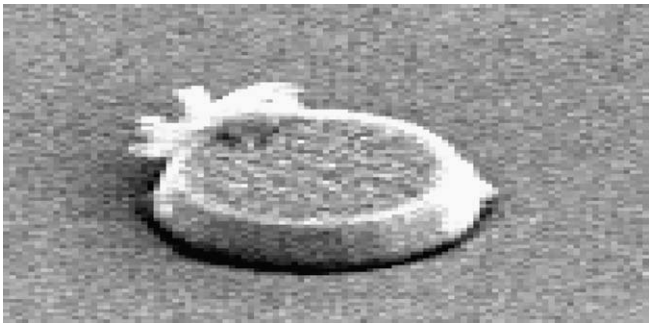

Fig. 6. Photograph of the etched glass plate surface by SEM.

3.2. Measurement of thermal conductivity

3.2.1. Measurement method

The thermal resistance across the VIC's is determined using an instrument illustrated schematically in Fig. 7. This apparatus operates on the principle of the guarded thermal hot plate [6]. The block heater is enclosed, with a very small gap, by a guard which is also in a good thermal contact with the sample and is maintained at a constant hot temperature T_h. The other side of the sample is maintained at a cold temperature T_c. The electric power supplied to the block heater is accurately measured and controlled so that it remains at T_h. When the block heater temperature is equal to the surrounding guard temperature, no heat flow occurs between the block heater and the guard, and all of the thermal power supplied to the block heater flows vertically through the sample. Then, the effective thermal conductivity k_{eff} is obtained from the thermal power Q.

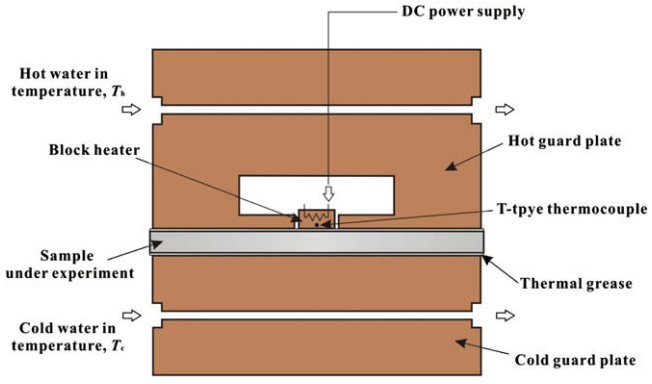

Fig. 7. Schematic diagram of the hot guarded plate.

$$k_{exp,efff} = \frac{Q \cdot L}{A_{eff} \cdot (T_h - T_c)} \tag{32}$$

The effective area of block heater A_{eff} is equal to the area surrounded by the mid-line of the gap between the block heater and the guard. In addition, it should be noted that $k_{exp,eff}$ may be either evaluated at the chip level or at the chip and vacuum envelop level. The chip thickness L_{chip} is 1.88 mm and the envelop thickness L_{env} is 1.25 mm. What we actually measure using the guarded plate apparatus(GPA) is $k_{exp,eff}$ at the chip and vacuum envelop level. However, since the chip level $k_{exp,eff}$ is more meaningful, we subtract the temperature drop at the envelope to have

$$k_{exp,\ eff@chip} = \frac{Q \cdot L_{chip}}{A_{eff}\left(T_h - T_c - \frac{Q \cdot L_{env}}{A_{eff} k_{env}}\right)} \tag{33}$$

where k_{env} is the thermal conductivity of the envelop material. Hereafter $k_{exp,eff}$ means $k_{exp,eff@chip}$.

The other details of the measurement system are further described here. All of the three parts, i.e., the block heater, the cold and hot guard plates are made of highly conducting copper to maintain isothermality in each of them. The block heater has diameter 28 mm and thickness 10 mm. The constant-voltage power supply to heat it has the accuracy of 0.05% in voltage and 0.15% in current. The guard diameter is 100 mm and the gap between block heater and guard is 2 mm. The constant temperatures on the hot and cold sides of the apparatus are maintained with JEIO TECH CW-10G/RW-0525G water bath circulator which have a specified temperature stability of ±0.1 °C and accuracy of ±0.05 °C. A data logger (Agilent, 34970 A) is used for reading the temperature of block heater. The measurement apparatus is then installed in a vacuum jar as shown in Fig. 8. The vacuum bell jar system has a cascade of a mechanical pump and a diffusion pump which have pumping speeds 3.3 and 570 l/s, respectively. It can be obtained the vacuum level of $0.13–1.33 \times 10^{-3}$ Pa (N/m^2). The system also has a TPG 251 A Pfeiffer vacuum gauge together with a PG105U Pirani vacuum gauge.

3.2.2. Performance test results

First of all, to verify the reliability of the constructed apparatus, a polystyrene sample with known thermal conductivity is taken as the reference and its thermal conductivity is measured several times. The measurement is made in an accredited thermal conductivity measuring equipment (NETZSCH, HFM436). The GPA-measurements are compared with those of reference [17] and the accredited equipment in Table 4. As shown in the table, the GPA results agree well with the others. The relative errors are less than 7.3% for all cases.

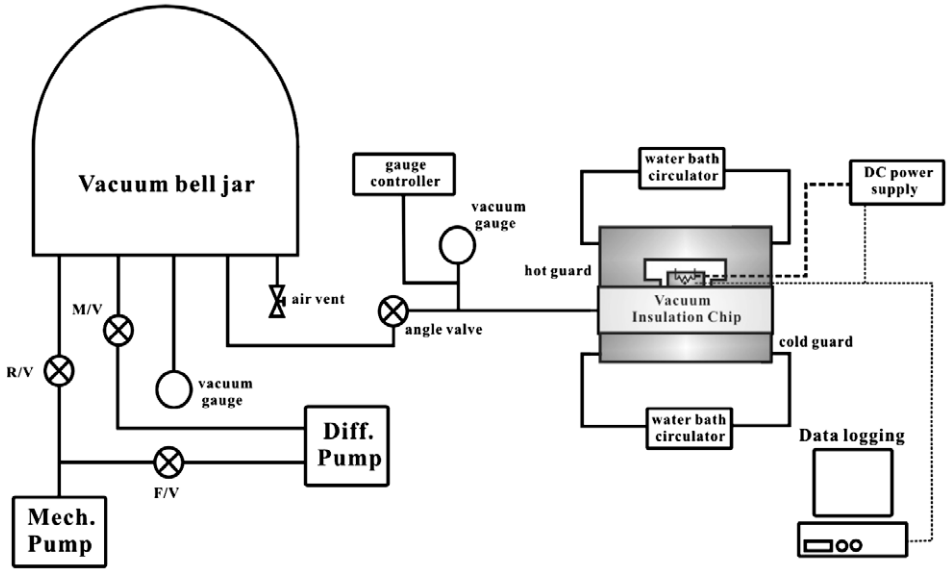

Fig. 8. Measurement apparatus of the chip thermal resistance.

Table 4
Experimental results of the polystyrene (10 mm thick) using the guard plate (T_c = 10 °C)

$T_h - T_c$ (°C)	GPA-measured thermal conductivity (W/m K)	Reference thermal conductivity (W/m K) [17]	Thermal conductivity obtained from the accredited equipment (W/m K)
15.0	0.0349	0.033	0.034
30.0	0.0354	0.033	0.034

Table 5
Effective thermal conductivity of VIC

Pressure (N/m^2)	$T_h - T_c$ (°C)	Effective thermal conductivity (W/m K)	
		Experiment	Calculation
1.33	30.0	0.0015	0.0014
	40.0	0.0015	0.0014
0.24	30.0	0.001	0.0009
	40.0	0.001	0.0009

We further conduct an uncertainty analysis. The total uncertainty dk of the measured quantity k as a function of Q,L,A,T_h, T_c (i.e., $k = f(Q,L,A,T_h,T_c)$) can be estimated using [18],

$$dk = \sqrt{\left(\frac{\partial k}{\partial Q}dQ\right)^2 + \left(\frac{\partial k}{\partial L}dL\right)^2 + \left(\frac{\partial k}{\partial A}dA\right)^2 + \left(\frac{\partial k}{\partial T_h}dT_h\right)^2 + \left(\frac{\partial k}{\partial T_c}dT_c\right)^2} \quad (34)$$

The uncertainties of L,A,T_h, and T_c are negligible compared with that of Q in this work. The uncertainty of Q is 5.0% for ΔT = 15 °C and 5.4% for ΔT = 30 °C at a 95% confidence level and these are the very uncertainties in k.

Thermal conductivity of VIC is measured at two different vacuum levels 1.33 and 0.24 Pa (N/m^2). Both levels are in free molecular flow regime, however, they simulate initial and deteriorated vacuum levels. The cold temperature is maintained at 5 °C. Table 5 shows the measured and the calculated effective thermal conductivity based on Eq. (31). The total uncertainty in k is less than 7.2% for all cases.

It is shown that the effective thermal conductivity of the chip is about 1/20 to 1/30 of conventional insulation materials. Air leakage up to 1.33 Pa (N/m^2) is shown to be acceptable. This is a practically useful insulation performance and it can be directly applied to a micro thermal chip. High temperature applications to such as fuel cells are also possible. Yet further improvement may be made by properly designing the plate, which has large portion of parts subject to light loading, meaning excessive thickness and good (thus, poorly insulating) thermal conduction. Collateral problems are vacuum maintenance, thermal expansion and thermal bridging to name a few. More research and development in this area are called for.

4. Conclusion

In the present work, theoretical and experimental analyses are made, aiming at the development of a VIC that has a low effective thermal conductivity. A conceptual design is proposed using LCD glass and vacuum gap, with staggered support legs. The actual parameters are obtained through the analyses of radiation, gas and support leg conductions. The results are cross-checked through commercial programs.

VIC's with three plates and two gaps are manufactured. Support legs are formed by etching and aluminum is coated on the two surfaces of the middle glass plate. Also, guarded hot plate to measure the effective thermal conductivity is constructed and the performance is validated.

The effective thermal conductivity of VIC is measured to be 0.0015 and 0.001 W/m K at 1.33 and 0.24 Pa (N/m^2), respectively. The current performance is good enough for practical applications and further improvements are yet possible.

Acknowledgements

This work was supported by the Korea Science and Engineering foundation (KOSEF) grant funded by the Korea government (MOST) (No. R01-2005-000-10682-0 (2007)) and the second stage of the Brain Korea 21 Project in 2007.

References

[1] M. Spinnler, E.R.F. Winter, R. Viskanta, T. Sattelmayer, Theoretical studies of high-temperature multi-layer thermal insulations using radiation scaling, J. Quant. Spectrosc. Radiat. Transfer 84 (2004) 477–491.

[2] M. Spinnler, E.R.F. Winter, R. Viskanta, Studies on high-temperature multilayer thermal insulations, Int. J. Heat Mass Transfer 47 (2004) 1305–1312.
[3] R.G. Scurlock, B. Saull, Development of multilayer insulations with thermal conductivities below 0.1 $\mu W\,cm^{-1}\,K^{-1}$, Cryogenics 16 (1976) 303–311.
[4] C.K. Krishnaprakas, K.B. Narayana, P. Dutta, Heat transfer correlations for multilayer insulation systems, Cryogenics 40 (2000) 431–435.
[5] S. Jacob, S. Kasthurirengan, R. Karunanithi, Investigations into the thermal performance of multilayer insulation (300–77 K) Part 2: thermal analysis, Cryogenics 32 (1992) 1147–1153.
[6] R.E. Collins, C.A. Davis, C.J. Dey, S.J. Robinson, J.Z. Tang, G.M. Turner, Measurement of local heat flow in flat evacuated glazing, Int. J. Heat Mass Transfer 36 (1993) 2553–2563.
[7] R.E. Collins, S.J. Robinson, Evacuated glazing, Solar Energy 47 (1991) 27–38.
[8] R.E. Collins, A.C. Fischer-Crips, J.Z. Tang, Transparent evacuated insulation, Solar Energy 49 (1992) 333–350.
[9] X.G. Liang, M.H. Han, Comparison of heat conduction and radiation of nano-size gaps, 1th International Conference on Microchannels and Minichannels, 2003, pp. 927–931.
[10] M.D. Whale, E.G. Cravalho, Analysis of the enhancement of thermal radiation between closely-spaced surfaces due to microscale phenomena, Natl. Heat Transfer Conf. 7 (1997) 41–50.
[11] M.D. Whale, E.G. Cravalho, Regimes of microscale radiative transfer for exchange of thermal energy between metallic surfaces, Natl. Heat Transfer Conf. 7 (1997) 65–72.
[12] M. Born, E. Wolf, Principles of Optics, seventh ed., Cambridge University, Cambridge, 1999.
[13] E.D. Palik, Handbook of Optical Constants of Solids, Academic, London, 1985.
[14] M.F. Modest, Radiative Heat Transfer, McGraw-Hill, New York, 1993.
[15] F.P. Beer, E.R. Johnston, Mechanics of Materials, 2nd ed., McGraw-Hill, London, 1995.
[16] A. Roth, Vacuum Technology, 3rd ed., Elsevier, Amsterdam, 1990.
[17] Y.S. Touloukian, Thermophysical properties of matter (Thermal conductivity : nonmetallic), Purdue University, Thermophysical Properties Research Center, 1970.
[18] J.P. Holman, Experimental Methods for Engineering, Addison-Wesley, New York, 1993.